J. Fluid Mech. (2001), *vol.* 441, *pp.* 255–264. Printed in the United Kingdom

Surface flow of granular materials: model and experiments in heap formation

By D. V. KHAKHAR[1], ASHISH V. ORPE[1], PETER ANDRESÉN[2] AND J. M. OTTINO[2]

[1]Department of Chemical Engineering, Indian Institute of Technology – Bombay, Powai, Mumbai 400076, India

[2]Department of Chemical Engineering, Northwestern University, Evanston, IL 60208, USA

(Received 18 May 2001)

Granular surface flows are important in industrial practice and natural systems, but the understanding of such flows is at present incomplete. We present a combined theoretical and experimental study of quasi-two-dimensional heap formation by pouring particles continuously at a point. Two cases are considered: open systems and closed systems. Experimental results show that the shear rate in the flowing layer is nearly independent of the mass flow rate, and the angle of static friction at the bed–layer interface increases with flow rate. Predictions of the model for the flowing layer thickness and interface angles are in good agreement with experiments.

1. Introduction

Surface flows of granular materials – thin layer flows on top of nearly quiescent granular beds – are important in industrial practice and nature. Industrial examples appear in the transportation, processing and storage of materials, in systems such as rotary kilns, tumbling mixers, and in feeding and discharge of silos. Examples in nature include formation of sand dunes, lava flow, avalanches, and transport of sediments in rivers. The simplest case corresponds to dry non-cohesive materials with air being the interstitial fluid and particles 100 μm and larger.

Experiments are relatively simple; the most straightforward way to produce a surface flow is by pouring grains on a heap. However, the understanding of surface flows is incomplete at present. Most of the emphasis has been on the theoretical side and several approaches, based on different physical assumptions have been proposed. Fluid mechanical approaches were pioneered by Bagnold (1954). Following this approach, Savage & Hutter (1989) developed a general model based on depth-averaged mass and momentum balance equations, assuming the flow to be purely frictional. At the other extreme we have *sandpile* cellular automata models and experiments, considering infinitesimally slow heap formation (Bak, Tang & Wiesenfield 1987; Frette *et al.* 1996).

There has been renewed activity in continuum descriptions in the past few years. Bouchaud *et al.* (1994) proposed a phenomenological continuum model for surface dynamics – now generally referred to as the BCRE model – based on the conservation of grains in the flowing layer and taking into account grains being *absorbed* into the stationary heap or *eroded* from the heap into the flowing layer. The momentum balance for grains is not explicitly considered. Instead, a form of the source term for

the rate of absorption or erosion of particles from the heap is assumed. For surfaces with small curvature, the source term is

$$\Gamma = \gamma R(\beta_r - \beta), \tag{1.1}$$

where R is the number density of flowing grains, β is the surface angle, β_r is the 'angle of repose' and $\gamma > 0$ is a phenomenological constant. Particles are absorbed into the heap if $\beta < \beta_r$ and the heap is eroded if $\beta > \beta_r$. Boutreux, Raphaël & de Gennes (1998) suggest that (1.1) is valid only for thin flowing layers. For thick layers relative to the particle diameter, they argue that the source term should be

$$\Gamma = V(\beta_n - \beta), \tag{1.2}$$

where $V \sim (gd)^{1/2}$ is a characteristic velocity, d is the particle diameter, and g is the acceleration due to gravity. Thus β_r is replaced by β_n, the *neutral angle*, the angle at which grains are neither absorbed nor eroded from the heap. Recently, Douady, Andreotti & Daerr (1999) developed a continuum model for heap formation following the approach of Savage & Hutter (1989), but allowing for exchange of grains between the heap and the layer. They found that the source term has the form (1.1) for thin layers and the form (1.2) for thick layers. Further, they obtained the velocity of grains in the layer to be proportional to the layer thickness, in contrast to the BCRE and Boutreaux *et al.* (BRdG) models where it is constant.

Although these models describe the qualitative behaviour of the system, quantitative predictions require the estimation of several phenomenological parameters, and this has not yet been done. The only related previous experimental works appear to be by Grasselli & Herrmann (1999), Grasselli *et al.* (2000) and Lemieux & Durian (2000). The dynamics of heap formation has not been studied by experiments in detail.

We note the parallel development of continuum models for free surface flows in partially filled rotating cylinders (Rajchenbach 1990; Rao, Bhatia & Khakhar 1991; Zik *et al.* 1994; Khakhar *et al.* 1997; Elperin & Vikhansky 1998; Makse 1999). In this case, the exchange of material between the fixed bed (which to a first approximation rotates as a solid body) and the layer of particles flowing on the surface is determined solely by kinematics and a model for the source term is not required. Other than this, however, the models for the two systems are nearly identical.

We present here an experimental study of quasi-two-dimensional heap formation by pouring particles continuously at a point. The systems considered are shown in figure 1, and denoted as *open systems* and *closed systems* using the terminology of Boutreux & de Gennes (1996). A continuum model for surface granular flow is developed along the lines of the boundary layer approach used previously for rotating cylinders (Khakhar *et al.* 1997). The plan of the paper is as follows. The model is developed in the following section and results for different limiting cases are discussed. Experimental details are given in § 3 and experimental results and comparisons to theory are given in § 4, with conclusions in § 5.

2. Theory

We consider a flowing layer on the surface of a heap (figure 1) assuming the flow is nearly uni-directional in the layer and curvature effects are small. The depth-averaged equations for flow in the layer are then the continuity equation

$$\frac{\partial}{\partial t}(\delta\langle\rho\rangle) + \frac{\partial}{\partial x}(\delta\langle\rho v_x\rangle) = (\rho v_y)|_{y=0}, \tag{2.1}$$

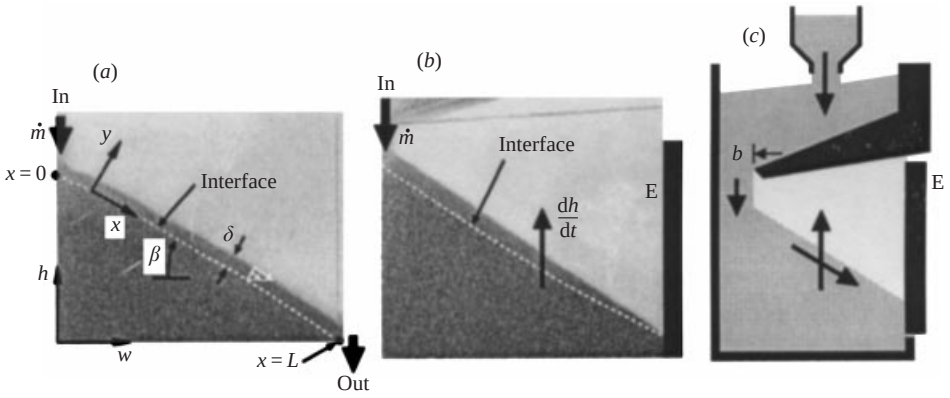

FIGURE 1. Typical streakline photographs showing the free surface profile and the heap–layer interface marked by a dashed line for (*a*) the open system and (*b*) the closed system. (*c*) A schematic view of the experimental apparatus. The endwall (E) is removed for the open heap experiments.

and the x-momentum balance equation

$$\frac{\partial}{\partial t}(\delta\langle\rho v_x\rangle) + \frac{\partial}{\partial x}(\delta\langle\rho v_x^2\rangle) = -\frac{\partial}{\partial x}(\delta\langle\tau_{xx}\rangle) + \tau_{xy}|_{y=0} + (\rho v_x v_y)|_{y=0} + \langle\rho\rangle g\delta\sin\beta. \quad (2.2)$$

In the above equations, v_x and v_y are the velocity components, τ_{xy}, τ_{xx} the shear stress and normal stress, ρ the bulk density of solids, $\beta(x,t)$ is the angle made by the interface with the horizontal, and $\langle\cdot\rangle = (1/\delta)\int_0^\delta \cdot\, \mathrm{d}y$ denotes average across the layer.

We make a number of assumptions to simplify (2.1)–(2.2). The bulk density in the layer (ρ) is taken to be nearly constant since the dilation of the flowing particles is small in the slow flows of interest here. The velocity profile in the layer is assumed to be linear and of the form

$$v_x = 2u(x,t)y/\delta, \quad (2.3)$$

where $u = \langle v_x\rangle$ is the depth-averaged velocity in the layer. Experimental studies of surface flows in rotating cylinders using particle tracking velocimetry show a more complex behaviour (Jain, Ottino & Lueptow 2001); however, here we take a linear profile for simplicity. The variation of the normal stress (τ_{xx}) in the flow direction (x) is neglected since changes in the layer thickness are small. The shear stress is taken to be a linear sum of the Bagnold collisional stress and the Coulombic frictional stress

$$\tau_{xy}|_{y=0} = -c\rho d\delta\left(\frac{\partial v_x}{\partial y}\right)^2 - \rho g\delta\cos\beta\ \tan\beta_s \quad (2.4)$$

where $c \approx 1.5$ is a parameter of the model and $\tan\beta_s$ is the effective coefficient of dynamic friction, with β_s taken to be the static angle of repose. The stress equation (2.4) is empirical and was obtained from an experimental study of surface flow in a rotating cylinder (Orpe & Khakhar 2001). With the above assumptions, the governing equations reduce to

$$\frac{\partial\delta}{\partial t} + \frac{\partial}{\partial x}(\delta u) = -\Gamma, \quad (2.5)$$

$$\frac{\partial}{\partial t}(\delta u) + \frac{4}{3}\frac{\partial}{\partial x}(\delta u^2) = -4cd\frac{u^2}{\delta} + g\delta\ \frac{\sin(\beta-\beta_s)}{\cos\beta_s}, \quad (2.6)$$

where $\Gamma = -v_y|_{y=0}$. To determine the location of the heap–layer interface an additional

condition is required. Assuming that the shear stress imposed by the flowing particles on the first layer of stationary particles in the heap (neglecting slow creeping motion, Komatsu *et al.* 2001) is balanced by friction, the Mohr–Coulomb criterion yields

$$\tau_{xy}|_{y=0} = -\rho g(\delta + d)\cos\beta \tan\beta_m, \tag{2.7}$$

where $\tan\beta_m$ is the effective coefficient of static friction. We refer to β_m as the 'maximum angle of repose' because it is the highest permissible angle under steady flow conditions. Using (2.4) and the assumptions given above, (2.7) reduces to

$$4cd(u^2/\delta) + g\delta\cos\beta\tan\beta_s = g(\delta + d)\cos\beta\tan\beta_m, \tag{2.8}$$

which gives a direct relation between the velocity in the layer (u) and the layer thickness (δ). For the case of thick layers ($\delta \gg d$) (2.8) simplifies to

$$u = \dot{\gamma}\delta/2, \tag{2.9}$$

with the shear rate ($\dot{\gamma} = \partial v_x/\partial y$) given by

$$\dot{\gamma} = \left[\frac{g\cos\beta\sin(\beta_m - \beta_s)}{cd\cos\beta_m\cos\beta_s}\right]^{1/2}. \tag{2.10}$$

Finally, the dynamics of the interface motion is given by

$$\frac{\partial h}{\partial t} = \Gamma\cos\beta, \quad \frac{\partial h}{\partial x} = -\sin\beta, \quad \frac{\partial w}{\partial x} = \cos\beta, \tag{2.11}$$

where $(h(x,t), w(x,t))$ gives the parametric equation for the interface (figure 1*a*). This completes the formulation of the model and all variables can be calculated using (2.5), (2.6), (2.9)–(2.11) and appropriate initial and boundary conditions.

The derivation given above is similar to that of Douady *et al.* (1999). An important difference between the two is that Douady *et al.* (1999) do not include a constitutive equation for stress in the flowing layer (equivalent to (2.4)). Instead, the velocity gradient in the flowing layer is assumed to be constant and given by $\dot{\gamma} = (g\sin\beta/d)^{1/2}$.

2.1. *Quasi-steady state solution*

Consider a quasi-steady flow ($\partial\delta/\partial t,\ \partial u/\partial t \approx 0$) in a thick flowing layer ($\delta \gg d$) and a slowly varying interface angle ($\partial\beta/\partial x \approx 0$). Using (2.9) and the above approximations, the continuity equation (2.5) becomes

$$\dot{\gamma}\delta\ \frac{\partial\delta}{\partial x} = -\Gamma, \tag{2.12}$$

and the momentum balance equation (2.6) together with (2.8) simplifies to

$$\dot{\gamma}^2\delta\ \frac{\partial\delta}{\partial x} = -\frac{g\sin(\beta_m - \beta)}{\cos\beta_m}. \tag{2.13}$$

Combining (2.12) and (2.13) yields

$$\Gamma = \frac{g\sin(\beta_m - \beta)}{\dot{\gamma}\cos\beta_m}, \tag{2.14}$$

which, for the case when $\beta_m \approx \beta$, reduces to

$$\Gamma \approx V(\beta_m - \beta), \tag{2.15}$$

where $V = g/\dot{\gamma}\cos\beta_m$. From (2.10) we get $\dot{\gamma} \propto (g/d)^{1/2}$ so that $V \propto (gd)^{1/2}$ as assumed in the BRdG model. Thus (2.15) is similar to the source term of the BRdG model, if we take the neutral angle to be the maximum angle of repose.

2.2. *Heap flow in an open system*

Consider the heap flow in an open system between vertical parallel plates separated by a gap T due to a continuous inflow of grains at one edge (figure 1*a*). At steady state, particles are neither absorbed nor eroded. Thus $\Gamma = 0$, which on substituting into (2.14) yields $\beta = \beta_m \equiv$ constant. The interface profile is obtained from (2.11) as $h(w) = h(0) - w \tan \beta_m$. Further, (2.12) and (2.13) indicate that in this case u and δ are constant along the layer. The mass flow rate is $\dot{m} = \rho u \delta T$, and using (2.9) we find that the layer thickness varies with the mass flow rate according to

$$\delta = [2\dot{m}/(T\rho\dot{\gamma})]^{1/2}. \tag{2.16}$$

2.3. *Formation of a heap in a closed system*

At steady state we must have $\mathrm{d}h/\mathrm{d}t \equiv$ constant for the heap to rise uniformly. Thus, the time variation of the interface is given by $h(x,t) = h(0,0) - \tan\beta w + \Gamma t \cos\beta$. Integrating (2.12), the layer thickness profile is obtained as

$$\delta = [\delta_L^2 + 2\Gamma(L-x)/\dot{\gamma}]^{1/2} \tag{2.17}$$

where δ_L is the layer thickness at the end of the layer given by $x = L$, and L is the length of the interface (figure 1*b*). A linear variation of layer thickness with distance was obtained by Boutreux & de Gennes (1996) assuming a constant velocity along the layer (u). The rise velocity is related to the mass flow rate by

$$\Gamma = \dot{m}/(TL\rho). \tag{2.18}$$

and the interface angle calculated from (2.15) is

$$\beta = \beta_m - \Gamma/V. \tag{2.19}$$

3. Experiments

3.1. *Materials and apparatus*

Experiments are carried out in a quasi-two-dimensional bin with vertical, transparent PMMA walls separated by a gap $T = 10\,\mathrm{mm}$. The bin is sufficiently tall and the upper part acts as the hopper as shown in figure 1(*c*). An auxiliary hopper is fitted on top of the bin to ensure that the supply hopper is full during an experimental run. The mass flow rate into the system is controlled by adjusting the gap width b at the exit of the hopper. The vertical height of the exit can also be adjusted. The same apparatus is used for the open and closed systems. In the open systems the endwall (E; see figure 1*c*) is removed. Steel balls of diameter $2 \pm 0.2\,\mathrm{mm}$ are used in the experiments. A few results are also reported for 1 mm steel balls.

3.2. *Open system experiments*

The objective of the experiments in the open system is to measure the interface angle and the layer thickness for different mass flow rates. The interface angle is of particular significance in this case since it is equal to the maximum angle of repose ($\beta = \beta_m$). The mass flow rate is directly measured by collecting the particles leaving the system for a fixed interval of time. Time lapse photography, in which the camera shutter is kept open for a sufficient interval (1/30 s) to obtain flow streaklines, is used to determine the layer thickness and the interface angle.

The height of the exit is adjusted so that the exit point is about 2–3 cm from the top of the heap to prevent bouncing of the particles when they fall on the

heap. The free surface of the flowing layer and the interface between the heap and the layer identified as the boundary between the moving particles (fuzzy) and the stationary particles (sharp) are traced manually on digitized streakline photographs using image analysis (Image Pro). Figure 1(*a*) shows a typical streakline photograph with the interface marked. The method allows measurement of the interface position to an accuracy of one particle diameter. Straight lines are fitted to the traced data points (after eliminating entrance and exit regions), and the interface and free surface angles are obtained from the slope of the line. The static angle of repose (β_s) is the surface angle when the particles have run out and the flow stops. In all the cases studied, the lines corresponding to the interface and free surface were nearly parallel indicating that the layer thickness is constant. The layer thickness is thus obtained as the difference between the intercept values for the two fitted lines. The variation of the mass flow rate with exit gap width (b; see figure 1*c*) is linear and was determined to be $\dot{m} = 22.7(b - 4.3)\,\mathrm{g\,s^{-1}}$, with b in mm.

3.3. *Closed system experiments*

The measurements for the closed system include the heap rise velocity ($\mathrm{d}h/\mathrm{d}t$), the layer thickness profile ($\delta(x)$) and the interface angle profile ($\beta(x)$) for different mass flow rates ($\dot{m}$). The heap rise velocity is measured from video recordings of the heap formation process, and the layer thickness profile and the interface angle profile are obtained by streakline photography. The mass flow rate is obtained from measurements of the exit gap width (b) using the fitted equation from the open system experiments.

The procedures used in the closed system experiments are similar to those for the open system. The distance that the particles free-fall at the entry point reduces as the heap rises. To minimize the bouncing of particles, the streakline photographs are taken only when the top of the heap has risen to about 3 cm below the exit. The height of the heap, measured near the middle ($x \approx L/2$), showed a linear increase with time over the entire duration of heap rise, in all the cases studied. Straight line fits to the data are used to obtain the heap rise velocity ($\mathrm{d}h/\mathrm{d}t$), which is independent of position along the interface (x). The coordinates of the free surface and interface are extracted from streakline photographs (see for example, figure 1*b*) using image analysis and fourth-degree polynomials are fitted to the data. The layer thickness profile ($\delta(x)$) and the interface angle profile ($\beta(x)$) are computed from the fitted polynomials.

4. Results and discussion

4.1. *Open system experiments*

The key result of the open system experiments is shown in figure 2(*a*). The data indicate that β_m, and thus the coefficient of static friction at the heap–layer interface ($\tan\beta_m$), is not a constant but increases with the local flow rate. The increase is greater for the smaller particles. The angles obtained for heap flow match those for a rotating cylinder when the flow rate is held constant (Orpe & Khakhar 2001). An increase in surface angle with flow rate was also reported by Lemieux & Durian (2000). Zhang & Campbell (1992) found the Mohr–Coulomb criterion with a constant coefficient of friction to be valid in their two-dimensional simulations of sheared spheres in a gravity field. Daerr & Douady (1999) reported an exponential decrease in the coefficient of static friction with height for particles at rest. Since the maximum angle

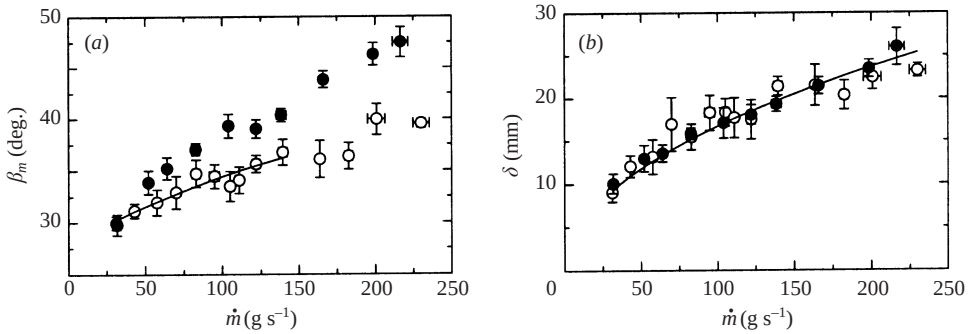

FIGURE 2. Variation of (*a*) the maximum angle of repose (β_m) and (*b*) layer thickness (δ) with mass flow rate ($\dot{m}$) for flow in an open system. Error bars indicate the standard deviation for ten measurements. Filled symbols: data for 1 mm steel balls, open symbols: data for 2 mm steel balls. Solid line in (*a*) is a fitted second-order polynomial spanning the range of mass flow rates used in the closed system experiments. Solid line in (*b*) is a fit of (2.16).

of repose varies by as much as 20° over the flow rates studied, neglecting the variation in the maximum angle with flow rate could result in significant errors in predictions.

Figure 2(*b*) shows the variation of the layer thickness (δ) with mass flow rate. It ranges from 10 mm to 20 mm for the flow rates studied and is nearly independent of particle size. The solid line is a fitted curve of the form $\delta \propto \dot{m}^{1/2}$. This suggests agreement with theoretical predictions (2.16) if the product $\rho\dot{\gamma}$ is independent of mass flow rate. As shown below, closed system experiments for 2 mm particles indicate that the bulk density is independent of mass flow rate and given by $\rho = 3.2\,\mathrm{g\,cm^{-3}}$. Using this value (which is justified since the local flow in the layer in the open and closed systems is very similar) we find from (2.16) that the shear rate is nearly constant, with $\dot{\gamma} = 22 \pm 3\,\mathrm{s^{-1}}$ for the 2 mm particles. The predicted shear rate using (2.10) and experimental values of β_m and β_s give $\dot{\gamma} = 20 \pm 5\,\mathrm{s^{-1}}$, which is in good agreement with the experimental value. The scaling used by Douady *et al.* (1999) gives $\dot{\gamma} = 53\,\mathrm{s^{-1}}$.

4.2. *Closed system experiments*

The closed system experiments show a linear dependence between heap rise velocity (Γ) and mass flow rate ($\dot{m}$), which is in concurrence with (2.18) if ρ is constant. A best fit line yields $\rho = 3.2\,\mathrm{g\,cm^{-3}}$. Figure 3 shows the variation of the layer thickness with distance from the end of the layer ($L - x$). The thickness at the end of the layer is nearly zero ($\delta_L \approx 0$) for the low flow rates; however, with increasing mass flow rates it increases monotonically with flow rate. In the case of wider bins or lower mass flow rates, the flowing layer would end away from the far edge of the bin and result in an intermittent flow. The solid lines in figure 3 are fits of (2.17) to obtain δ_L and $\dot{\gamma}$. There is a good match between the fitted lines and the experimental data, which implies that the shear rate, $\dot{\gamma}$, is nearly constant. Using experimental results for the rise velocity (Γ) and the interface length (L), we obtain $\dot{\gamma} = 20 \pm 2\,\mathrm{s^{-1}}$, where the standard deviation indicated is calculated for all 10 flow rates studied. Thus the shear rates for the open and closed systems are the same within experimental error.

The angle of the interface also varies with distance along the interface. Results obtained from analysis of the streakline photographs are shown in figure 4. Although the angle is roughly constant in the middle region, there is a significant decrease with distance from the pouring point. This picture is different from the result predicted

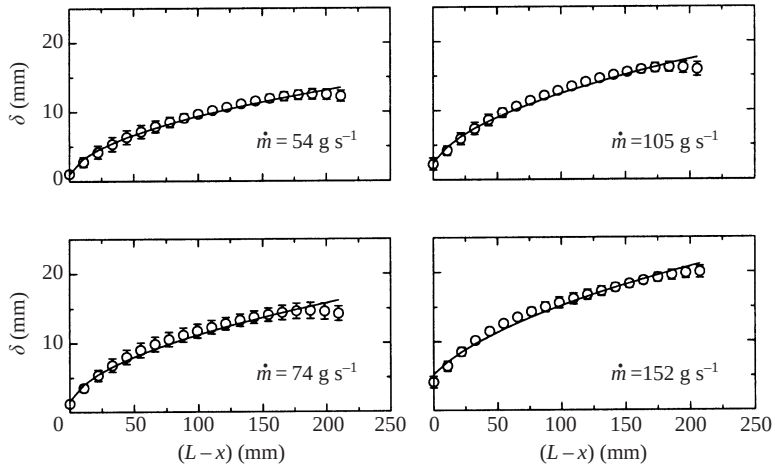

FIGURE 3. Variation of the layer thickness (δ) with distance from the end of the layer ($L-x$) for ten different mass flow rates in a closed system. Symbols show experimental data for 2 mm steel balls and error bars indicate the standard deviation over six measurements. Solid lines are fits of (2.17).

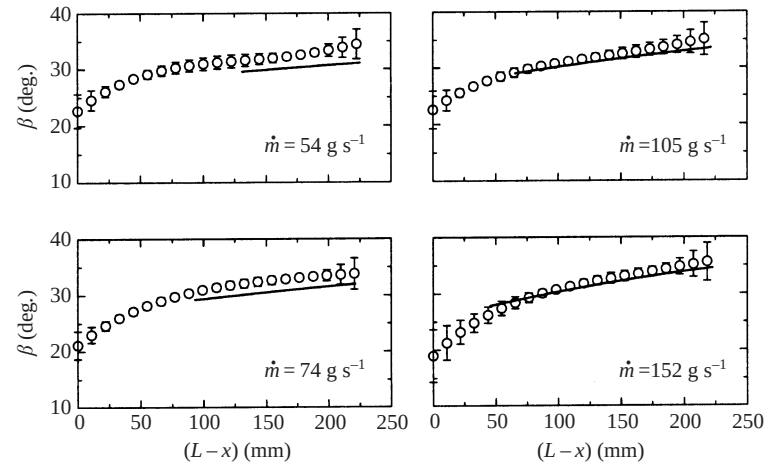

FIGURE 4. Variation of the interface angle (β) with distance from the end of the layer ($L-x$) corresponding to the data in figure 3. Solid lines are predictions of (2.19).

by Boutreux & de Gennes (1996) in which the interface angle was found to be a constant.

Comparison of the interface angle profile to theoretical predictions requires an estimate of the maximum interface angle (β_m) for the closed system. Here we assume that the maximum angle is determined by the local flow rate and use the data obtained for the open system to determine a correlation between β_m and $\dot{m}$. A second-degree polynomial is fitted for a range of mass flow rates corresponding to those used in the closed system experiments (solid line in figure 2*a*). Since the density in the layer (ρ) is constant and the heap rise is uniform (Γ = constant), the mass flux transferred from the layer into the heap is uniform along the interface. Thus the mass flow rate varies linearly with distance and is given by $\dot{m}_x = \dot{m}(1-x/L)$. The maximum angle of repose at any position is then calculated as $\beta_m = \beta_m(\dot{m}_x)$ using the fitted polynomial, and β from (2.19). Predictions shown in figure 4 indicate good agreement between theory

and experiment at the higher flow rates; at low flow rates there are some differences between the two. The predictions span only the mass flow rate range of the fitted curve shown in figure 2(*a*).

5. Conclusions

Experimental results for open and closed systems give new insight into granular surface flows. Measurements of the surface angle in the open system directly yield the angle of static friction (β_m) which increases with the mass flow rate. The layer thickness is found to increase with mass flow rate as $\delta \propto \dot{m}^{1/2}$. Closed system experiments show that the heap rise velocity is directly proportional to the mass flow rate of particles, implying that the bulk density is nearly constant in the flowing layer. Further, the layer thickness varies as $\delta^2 \propto x$ and the interface angle decreases with distance from the pouring point.

Model predictions are, by and large, in good agreement with experimental results using fitted values for the two parameters: the bulk density and shear rate. Both are found to be independent of the mass flow rate for the ranges of $\dot{m}$ studied. The shear rate is also found to be nearly same for the open and closed systems. The shear rate predicted from theory is nearly constant as well, and equal to the fitted values. The results presented here are robust, and represent a subset of a much wider range of experimental studies carried out. Similar results are obtained for different materials (1 mm steel balls, and glass beads of different sizes) and for systems with different geometry.

Quasi-two-dimensional experiments are becoming a common element in the tool-kit of granular flow investigations. A question common to quasi-two-dimensional studies is the extent to which walls affect the results. Undoubtedly density is affected. However, to the extent that the walls are not accounted for explicitly in the models a few comments are in order. To a first approximation the effect of walls may be quantified by the ratio of particle diameter, d, to the thickness of the container, T. The experiments reported here were conducted with d/T in the range 5 to 10, and results are qualitatively similar for different ratios. For example, the layer thickness–mass flow rate curve is nearly independent of d/T. Another set of investigations relevant to the discussion are those in rotating cylinders. The evidence emerging from these studies is that the flowing layers are relatively unaffected by d/T in the range 5 to 25 (Orpe & Khakhar 2001; Jain *et al.* 2001). A possible way to justify this is in terms of the ratio of energy dissipation due to wall friction ($\dot{\gamma}\delta \tan\beta_w N$, where $\tan\beta_w$ is the coefficient of wall friction and $N \sim \rho g \delta \cos\beta$ is the characteristic normal stress), to the energy dissipation in the flow ($\dot{\gamma} \tan\beta_m N T$), both for unit wall area. In the dilated flowing layer the resistance will be due to rolling friction – $\beta_w \sim 2^\circ$ – for which the ratio is 0.04. However, near the interface the resistance will be due to sliding friction – $\beta_w \sim 12^\circ$ – for which the ratio is 0.3. In any case, this signals the beginning of the questions that should be asked and not the end. Clearly more extensive research should be carried out to elucidate the effects of the d/T and the absolute influence of d.

This work was supported in part by grants to J. M. O. from the Division of Basic Energy Sciences of the Department of Energy, the National Science Foundation, Division of Fluid and Particulate Systems, and the Donors of the Petroleum Research Fund, Administered by the American Chemical Society. D. V. K. acknowledges the

financial support of the Department of Science and Technology, India, through the Swarnajayanti Fellowship project (DST/SF/8/98) for part of this work.

REFERENCES

Bagnold, R. A. 1954 Experiments on a gravity-free dispersion of large solid spheres in a Newtonian fluid under shear. *Proc. R. Soc. Lond.* A **255**, 49–63.

Bak, P., Tang, C. & Wiesenfeld, K. 1987 Self-organized criticality: An explanation of the 1/f noise. *Phys. Rev. Lett.* **59**, 381–384.

Bouchaud, J. P., Cates, M. E., Prakash, J. R. & Edwards, S. F. 1994 A model for the dynamics of sandpile surface. *J. Phys. Paris* I **4**, 1383–1410.

Boutreux, T. & Gennes, P. G. de 1996 Surface flows of granular mixtures: I. General principles and minimal model. *J. Phys. Paris* I **6**, 1295–1304.

Boutreux, T., Raphaël, E. & Gennes P. G. de 1998 Surface flows of granular materials: A modified picture for thick avalanches. *Phys. Rev.* E **58**, 4692–4700.

Daerr, A. & Douady, S. 1999 Two types of avalanche behaviour in granular media. *Nature* **399**, 241–243.

Douady, S., Andreotti, B. & Daerr, A. 1999 On granular surface flow equations. *Eur. Phys. J.* B **11**, 131–142.

Elperin, T. & Vikhansky, A. 1998 Granular flow in a rotating cylindrical drum. *Europhys. Lett.* **42**, 619–623.

Frette, V., Christensen, K., Malthe-Sorensen, A., Feder, J., Jossang, T. & Meakin, P. 1996 Avalanche dynamics in a pile of rice. *Nature* **379**, 49–52.

Grasselli, Y. & Herrmann, H. J. 1999 Shapes of heaps and in silos. *Eur. Phys. J.* B **10**, 673–679.

Grasselli, Y., Herrmann, H. J., Oron, G. & Zapperi, S. 2000 Effect of impact energy on the shape of granular heaps. *Granular Matter* **2**, 97–100.

Jain, N., Ottino, J. M. & Lueptow, R. M. 2001 An experimental study of the flowing granular layer in a rotating tumbler. *Phys. Fluids* (in press).

Khakhar, D. V., McCarthy, J. J., Shinbrot, T. & Ottino, J. M. 1997 Transverse flow and mixing of granular materials in a rotating cylinder. *Phys. Fluids* **9**, 31–43.

Komatsu, T. S., Inagaki, S., Nakagawa, N. & Nasuno, S. 2001 Creep motion in a granular pile exhibiting steady surface flow. *Phys. Rev. Lett.* **86**, 1757–1760.

Lemieux, P.-A. & Durian, D. J. 2000 From avalanches to fluid flow: A continuous picture of grain dynamics down a heap. *Phys. Rev. Lett.* **85**, 4273–4276.

Makse, H. A. 1999 Continuous avalanche segregation of granular mixtures in thin rotating drums. *Phys. Rev. Lett.* **83**, 3186–3189.

Orpe, A. V. & Khakhar, D. V. 2001 Scaling relations for granular flow in quasi-two-dimensional rotating cylinders. *Phys. Rev.* E (in press).

Ottino, J. M. & Khakhar, D. V. 2000 Mixing and segregation of granular materials. *Ann. Rev. Fluid Mech.* **32**, 55–91.

Rajchenbach, J. 1990 Flow in powders: From discrete avalanches to continuous regime. *Phys. Rev. Lett.* **65**, 2221–2224.

Rao, S. J., Bhatia, S. K. & Khakhar, D. V. 1991 Axial transport of granular solids in rotating cylinders. Part 2: Experiments in a non-flow system. *Powder Technol.* **67**, 153–162.

Savage, S. B. & Hutter, K. 1989 The motion of a finite mass of granular material down a rough incline. *J. Fluid Mech.* **199**, 177–215.

Zik, O., Levine, D., Lipson, S. G., Shtrikman, S. & Stavans, J. 1994 Rotationally induced segregation of granular materials. *Phys. Rev. Lett.* **73**, 644–647.

Zhang, Y. & Campbell, C. S. 1992 The interface between fluid-like and solid-like behaviour in two-dimensional granular flows. *J. Fluid Mech.* **237**, 541–568.